

Density and magnetic fluctuations at JET: experimental observation and numerical characterization

**G. De Masi¹, I. Predebon¹, S. Spagnolo¹, I. Lupelli², J. C. Hillesheim², L. Meneses³,
E. Delabie⁴, C. Maggi² and JET Contributors^{*}**

EUROfusion Consortium, JET, Culham Science Centre, Abingdon, OX14 3DB, UK

¹Consorzio RFX, C.so Stati Uniti 4, 35127 – Padova, Italy

²CCFE, UK Atomic Energy Authority, Culham Science Centre, Abingdon, OX14 3DB, UK

*³Instituto de Plasmas e Fusão Nuclear, Instituto Superior Técnico, Universidade de Lisboa,
Lisboa, Portugal*

⁴Oak Ridge National Laboratory, Oak Ridge, Tennessee 37831-6169, USA

**See the author list of: X. Litaudon et al., Overview of the JET results in support to ITER, accepted for publication
in Nuclear Fusion*

Introduction. Pedestal conditions are of particular interest for tokamak physics and the study of the electromagnetic instabilities influencing its evolution is crucial to gain insight on this region. In this contribution we present a characterization of density and magnetic fluctuations experimentally observed on the JET pedestal top region and a subsequent numerical modeling

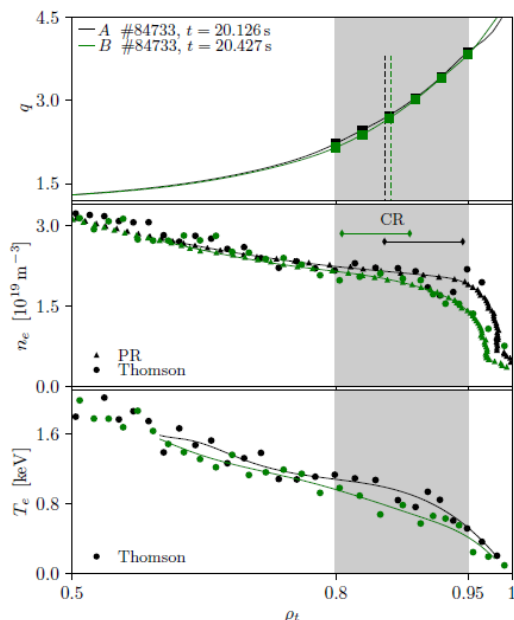


Fig. 1: q edge radial profile (top); edge n_e radial profile (middle); edge T_e radial profile (bottom). Black and green lines refers respectively to case A and B. Grey shaded region represents the CR measurement regions.

based on the real plasma equilibria.

Plasma scenario and experimental set-up. The analysis refers to a set of JET discharges performed to investigate the phenomenology of the LH transition and its link to the Scrape Off Layer and divertor conditions [1]. The experiments were designed with a slow power ramp in the Neutral Beam Injection (P_{NBI}) with toroidal field $B_\phi = 2.4$ T, plasma current $I_p = 2$ MA and $q_{95} = 3.5$. The divertor configuration was set to have both strike points on the vertical targets (VT configuration). Core density was scanned on a shot-to-shot basis in the range $n_e = [0.2-0.3] \times 10^{20} \text{ m}^{-3}$. In fig.1 we show two typical electron density and temperature edge radial profiles as measured after the LH transition

by the Profile Reflectometer (PR) and the High Resolution Thomson Scattering (HRTS). A clear pedestal arises only in the electron density, while electron temperature gradient is comparable to the L-mode case [2]. Nevertheless, after the transition, plasma edge is characterized by continuous type-III ELMs occurrence (see fig. 2d). Density fluctuations measurements are obtained through a correlation reflectometer (CR) composed by two X-mode W-band channels that can be independently controlled. In the discharge shown in this contribution, the first channel (master) was kept at a fixed frequency (the lowest available in the system, 73.44 GHz) corresponding to the density pedestal top (normalized poloidal flux $\Psi_N \approx 0.93$), while the second channel (slave) was swept over 13 difference frequencies every 0.2 ms starting by the master frequency and covering a broader radial region ($\Psi_N \approx [0.87-0.93]$). CR measurement positions are also shown in fig.1. Magnetic fluctuations measurements are obtained through two pairs (toroidally and poloidally separated) of pick-up coils being part of a high resolution coil array located in the low field side (LFS). All fluctuations data are digitally sampled at 2 MHz.

Density fluctuations. In fig.2a the spectrogram of the density fluctuations as measured by the CR master channel is shown. A broad band activity with a frequency peak around 70 kHz is rather evident during the whole time window. Its temporal behaviour reveals the intermittent nature of this activity. In particular, the fluctuations amplitude appears increasing in the inter-ELM phases (amplitude not shown) and seems to have a qualitative agreement with the local logarithmic electron temperature gradient $1/L_{Te}$ as measured by the

Electron Cyclotron Emission (ECE)

system. The analysis of the fluctuations data from the slave channels reveal a

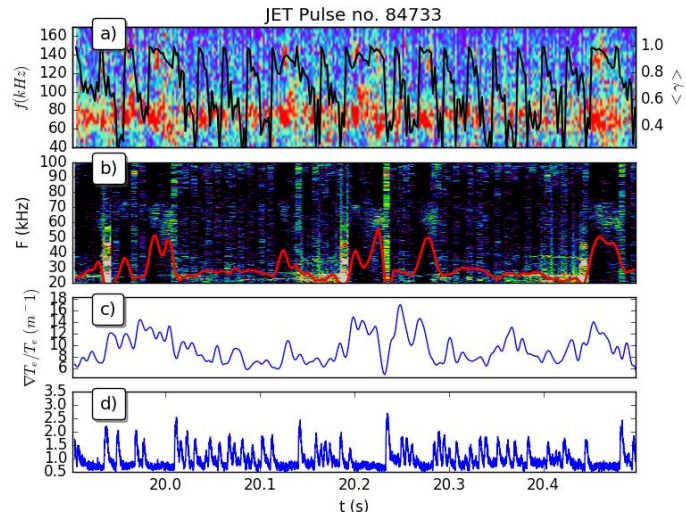


Fig.2: a) n_e fluctuations spectrogram and timetrace of the correlation γ (black) between the two CR channels; b) δb_0 spectrogram and integrated amplitude (red); c) timetrace of the local temperature gradient; d) timetrace of the BeII photon flux in outer divertor

similar activity (not shown here) also in the more internal regions, while we do not have information on the steep gradient region. In fig.2a the superimposed black line represents the time trace of the correlation γ between the two CR channels. In the inter-ELM phases $\gamma \approx 1$ and the associated correlation length can be estimated as $r_\gamma \approx 5-8$ cm. Moreover, by using a simple 1D model (power spectral density associated to this frequency range is almost one order of

magnitude over the background), we can estimate the amplitude of the associated density fluctuations: in the inter-ELM phases we find $\delta n_e/n_e \leq 2\%$.

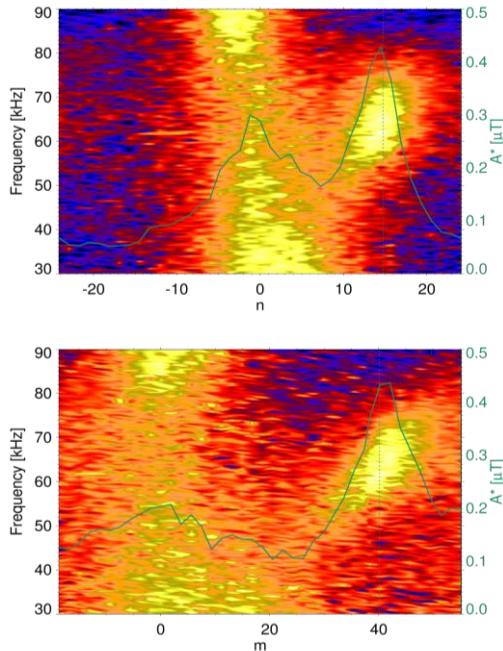


Fig.3: color coded (a.u.) $S(n,f)$ and $S(m,f)$ spectra. Right y-axis: fluctuations amplitude

activity. In fig.3 we report the spectra (averaged over the time window shown in fig.2) as a function of the frequency f and the poloidal and toroidal mode numbers (m and n , respectively). The oscillation frequency around 65 kHz is characterized by a poloidal mode number $m \sim [35, 45]$ and a toroidal mode number $n \sim [12, 17]$. The superimposed green curve represents the amplitude associated to this coherent structure taking into account the amplitude attenuation caused by the large size of the sensors [2]. Based on the above estimates, assuming they resonate, we expect these magnetic activity to be radially localized around the $q \sim [2.5-3]$ magnetic surface and, thus, according the EFIT++ equilibrium (fig.1), in the pedestal top region. Moreover, the integrated spectra $A^*(t)$ shown in fig.2b, shows a qualitative agreement with local logarithmic electron temperature gradient $1/L_{Te}$ evaluated at $\Psi_N \approx 0.93$. According to the m evaluation, the typical spatial scale of these fluctuations is in the range $0.01 < k_\theta \rho_i < 0.1$ (range of microinstabilities). Phase velocity can be estimated as $v_{ph,\theta} = \omega/k_\theta \approx 10$ km/s (in the electron diamagnetic direction).

Magnetic fluctuations. In fig.2b the spectrogram of the fluctuations of the poloidal component of the magnetic field, δb_θ , is shown. Among the others, an intermittent activity with a frequency of around 60-70 kHz can be observed in the time windows just preceding the ELM crashes. Also in this case, the superimposed red line represents the timetrace of the power spectral density $A^*(t)$ integrated in the frequency range [53, 74] kHz. A similar activity is detected by the whole high resolution coil array located in the LFS, while is not detected in the High Field Side (HFS) coils. The two-point technique [3] has been applied to the signals from two pairs of toroidally and poloidally separated coils in order to obtain information on the structure of the magnetic

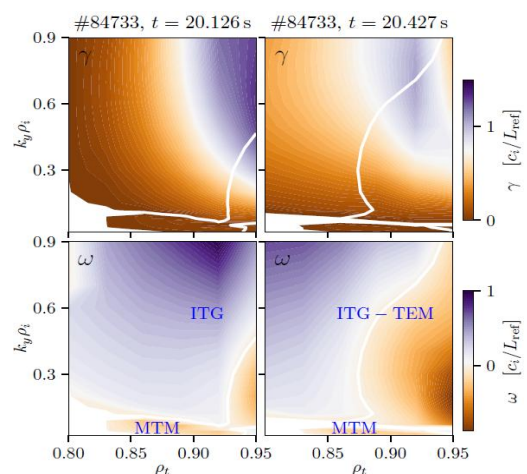


Fig4: Stability analysis in terms of growth rate γ (top) and real frequency ω (bottom) for case A (left) and case B (right) as a function of the radial coordinate ρ_t .

Numerical simulations. To gain insight on the stability issues of the observed turbulent activity, we rely on the gyrokinetic code GENE [4] applied to two realistic experimental cases (dubbed A and B), experimentally characterized by a respectively high/low fluctuations level. The related EFIT++ equilibria are very similar in terms of q profile and metric quantities, while the kinetic profiles are different (Fig.1). Further details on the simulations can be found in [2]. A radial scan in the pedestal top region corresponding to the CR measurement position and the $q \sim [2.5-3]$ surfaces is performed. Linear results (shown in fig.4) reveal the coexistence of different instabilities: mainly ion temperature gradients (ITG) modes for $0.1 < k_y \rho_i < 2$, micro-tearing modes (MTM) for $k_y \rho_i < 0.1$, electron temperature gradient (ETG) modes for $k_y \rho_i > 2$, and trapped electron modes (TEM) approaching the steep gradient region. According to the experimental findings, case A shows higher growth rates for ITG modes, and a slightly broader range in k_y of unstable MTMs. Preliminary non-linear simulations (electromagnetic, with realistic values of β and collisionality, plasma rotation not included) have been performed for case A in the pedestal top.

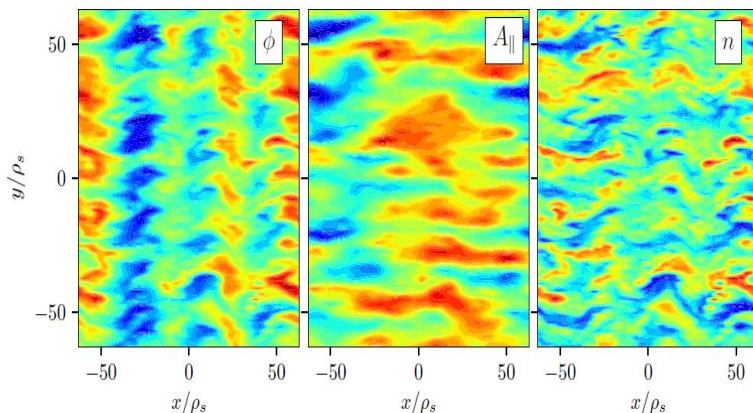


Fig.5: Contour plot, as a function of the normalized radial (x) and poloidal (y) coordinate, of electrostatic potential, vector potential, and density for case A

They show the presence of ITG turbulence with a mainly electrostatic ion heat/particle flux component, which is 2-3 times larger than the electron one, peaked around $k_y \rho_i \sim 0.3$. In Fig.5, we show a snapshot of saturated turbulence for the electrostatic and vector potentials, and density fluctuations in the (x,y) plane. Density fluctuations

turn out to be of the order of 1-2%, consistent with the experiments.

Discussion. In JET low β_e type-III ELM discharges, density and magnetic fluctuations located on the pedestal top have been experimentally characterized. They have a inter-ELM evolution and a link with local kinetic quantities. Numerical simulations suggested a possible interpretation in terms of ITG modes for density fluctuations, while magnetic fluctuations phenomenology needs to be further investigated.

References

- [1] H. Meyer et al., Proc. of the 41st EPS Conference, P1.013 (2014)
- [2] G. De Masi et al., to be submitted to Nuclear Fusion
- [3] J. M. Beall, Y. C. et al., J. Appl. Phys., 53 3933 (1982)
- [4] <http://www.genecode.org>

This work has been carried out within the framework of the EUROfusion Consortium and has received funding from the Euratom research and training programme 2014-2018 under grant agreement No 633053. The views and opinions expressed herein do not necessarily reflect those of the European Commission.